Cement & Concrete Composites 34 (2012) 328–336

Contents lists available at SciVerse ScienceDirect

Cement & Concrete Composites

journal homepage: www.elsevier.com/locate/cemconcomp

High volume limestone alkali-activated cement developed by design of experiment

Alexander J. Moseson [a,*], Dana E. Moseson [b], Michel W. Barsoum [c]

[a] Drexel University, Department of Mechanical Engineering & Mechanics, 3141 Chestnut Street, Randell Hall 115, Philadelphia, PA 19104, USA
[b] Emerson Resources, Inc., 600 Markley Street, Norristown, PA 19401, USA
[c] Drexel University, Department of Materials Science and Engineering, 3141 Chestnut Street, LeBow 344, Philadelphia, PA 19104, USA

ARTICLE INFO

Article history:
Received 17 August 2010
Received in revised form 7 September 2011
Accepted 11 November 2011
Available online 20 November 2011

Keywords:
Alkali activated cement
Granulated blast-furnace slag
Mixture proportioning
Mechanical properties
Limestone
Design of experiment

ABSTRACT

Herein, we report on the development of a cement comprising ground granulated blast furnace slag, soda ash (sodium carbonate), and up to 68 wt.% granular limestone. Mixture Design of Experiment (DOE) was utilized, with analysis of compressive strength, modulus of elasticity, hydraulic properties, cost, CO_2 production, and energy consumption. Models were derived to understand the impact of mix design on performance and for optimization. Successful formulations are hydraulic and cure at room temperature, with strengths as high as 41 MPa at 3 d and 65 MPa at 28 d. These formulations, compared to OPC, are competitive in cost and performance and can reduce both CO_2 production and energy consumption by up to 97%.

1. Introduction

The manufacture of one tonne of the Ordinary Portland Cement (OPC) generates 900 kg of CO_2 and requires 1510 kW h of energy [1]. While this is, on a unit weight basis, considerably less than other options like steel or treated wood, the enormous volume of cement produced (2.6 billion tons in 2007 [2]) is responsible for approximately 5% of global anthropogenic CO_2 production.

As environmental sustainability becomes a greater priority, solutions are being sought to reduce the CO_2 and energy burden of cement without sacrificing economic viability. These include emissions sequestration, concretes with lower OPC content, blends of OPC with pozzolans, magnesia cements, alumino-silicate based geopolymers, and more [3]. Efforts are also underway to measure the environmental impact of OPC and its alternatives, for example those introducing novel metrics such as binder intensity and CO_2 intensity [4], and those performing life cycle analysis [5].

Due in part to its low energy and CO_2 burdens, the use of limestone to replace OPC is an increasingly popular path [6,7]. Originally thought to be an inert filler, recent research has shown, to varying extents, limestone to be chemically and physically active in hydraulic cement [8]. Current standards allow a replacement, of up to 5 wt.% OPC in the US (ASTM C150-04) and up to 35 wt.% in Europe (EN-197-1-2000) [9]. Compared to the energy-intensive kiln-firing process of OPC, maximizing the use of limestone would be desirable to minimize environmental impact.

Another approach to ecological cement is that of geopolymer or alkali-activated cement (AAC), which generally use no OPC. Their advantages over OPC may include: (i) drastically less CO_2 production; (ii) longer life and better durability; (iii) better defense against chemical attack (e.g. chlorides, sulfates); (iv) rapid strength gain; (v) better performance in marine environments; and (v) repurposing of industrial waste [3,10–17].

The present work was designed to combine the two above approaches to develop high-volume limestone AACs. Analysis was conducted with respect to key characteristics of performance (strength, modulus, hydraulic stability) and economy and ecology (cost, CO_2 production, energy requirement). Design of Experiment (DOE), a statistical method of designing and analyzing multi-variable experiments, was used to extend earlier work [18–21]. Most statistical investigations of AACs have used factorial DOE, with typical variables being raw material specifications (e.g. specific slag surface areas), processing (e.g. curing temperature), categorical factors (e.g. activator chemical), and certain chemical ratios (i.e. amounts of activator) [22–27]. In contrast, this work relies on mixture DOE, thus focusing on the roles and interactions of the system components, and mixture optimization.

This study was intended not only to better understand the impact of mix design on high volume limestone AAC performance, but also to aid in the development of cements for markets in both developed and developing countries. Four ingredients were used: ground granulated blast furnace slag (GGBFS), granular limestone,

* Corresponding author. Tel.: +1 215 253 8484; fax: +1 215 895 6760.
E-mail address: AlexMoseson@Drexel.edu (A.J. Moseson).

0958-9465/$ - see front matter © 2011 Elsevier Ltd. All rights reserved.
doi:10.1016/j.cemconcomp.2011.11.004

sodium carbonate (Na_2CO_3), and water. These ingredients were chosen partially for their real-world practicality. For example, the limestone used was a widely available consumer-grade, granular limestone instead of lab-grade $CaCO_3$. Of common activators, Na_2CO_3 is one of the most ubiquitous, inexpensive, and environmentally benign. No admixtures or fibers were included and, hoping to leverage the advantages of AACs, no OPC. The result is novel high volume limestone AACs, which are competitive in performance with OPC, some of which have a CO_2 and energy consumption reductions approaching 100% instead of the more common Portland Cement Association (PCA) goal of 10 % [28].

2. Material and methods

2.1. Experimental methods

As noted above, four raw materials were used. The first was slag (GGBFS) (St. Lawrence Cement, Camden, NJ) with a Blaine fineness of 498 m^2/kg (as tested by the authors per ASTM C204-07 [29]). X-ray Fluorescence (XRF) analysis of the GGBFS was carried out by Arkema, Inc. in King of Prussia, PA (Table 1). Second is sodium carbonate, Na_2CO_3 (Brenntag Pacific, Inc., Santa Fe Springs, CA). Third is granular limestone with a $CaCO_3$ content of 89.3 wt.% and a $MgCO_3$ content of 10.7 wt.% (Oldcastle Stone Products, Atlanta, GA). The cumulative particle size distribution of the latter is: 23% < 75 μm, 48% < 150 μm, 68% < 300 μm, 100% < 1000 μm. Fourth, tap water.

A strict interpretation of ASTM C125-07 and ASTM C219-07a would, respectively, define the limestone used as a fine aggregate and the mixture as a mortar [30,31]. However, since the granular limestone in this case is chemically active [18,19], the material could be used as a cement, as it meets the ASTM definition for hydraulic cement, except for the limestone particle size. Nevertheless, henceforth it is labeled a hydraulic cement.

ASTM C192/C192M-07 guided the preparation of 2 in. × 4 in. cement paste (not mortar or concrete) cylinders for compression testing [32]. The four components were weighed, dry mixed, and the water added. The mixture was then mixed by hand for approximately 2 min. Each cylinder was half-filled and rodded in two lifts then struck off with a trowel. The two curing conditions, both at room temperature, were ASTM C192 standard 100% RH – henceforth referred to as moist cure - and submerged in a plain water bath (without lime), where the water was changed every 24 h to avoid possible equilibrium effects due to leaching.

Samples were stored in the molds for 24 h, covered by plastic sheets, after which they were removed from the molds and placed in their respective curing conditions until testing. The compressive strength was measured according to ASTM C39/C39M-09a, using unbonded rubber caps (ASTM C1231/1231M-10), on a load frame (Instron 5800R, Norwood, MA) [33,34]. The strain was measured using an extensometer and the modulus of elasticity calculated according to ASTM C469-02 [35]. For each age, 3 or 28 d, and curing condition, three cylinders were tested for each DOE run, and six for each validation run. The weight of each cylinder was measured immediately after removal from the mold and immediately before compression testing.

Cost, CO_2 production, and power consumption were calculated for each run. The bulk costs of components were determined from government and industry data, as listed in Table 2. The CO_2 production and power consumption were calculated from studies of cement production; details are provided in Appendix A. The costs, CO_2 production, and energy consumption for each component are listed in Table 2 [36–39].

2.2. Design of Experiment (DOE)

Prior to the DOE, initial one-factor-at-a-time (OFAT) experiments were performed to establish the system boundaries (Table 2) and to begin to understand the system's trends. Boundaries were intentionally wide to include unconventional ratios (e.g. up to 80 wt.% limestone), while still limited enough to provide sufficient detail for modeling. The boundaries represent ratios of Na_2CO_3 spanning hydraulic stability to detrimental leaching; ratios of water for spanning the limits of workability (very dry to very wet), and GGBFS and limestone (with equal boundaries) to produce strength in the range of OPC.

DOE experiment design and analysis was performed on Design-Expert v7.1.5 (Stat-Ease Inc., Minneapolis, MN). A D-optimal mixture design was used, with the four components for each run totaling a fixed weight of 6200 g. A special-cubic Scheffe model was used for the design in order to include tertiary interactions, if any were present. The design comprised 14 model points, 3 lack of fit points, 3 replicates, and 2 additional center points, for a total of 22 runs. In keeping with best practices of DOE, efforts were made to minimize variance, such as keeping the operator, preparation and curing procedures, and test equipment as consistent as possible for all runs.

To determine the model for each response, the model terms were determined by stepwise selection (α in and out: 0.10). Transformations were selected and outliers were removed, as appropriate, to generate the model with the highest statistical significance, determined by Analysis of Variance (ANOVA) and other diagnostic tools such as Box Cox, Cook's Distance, and Normal Plot of Residuals plots. Numerical optimization of variables and responses were performed by assigning criteria to each response as desired. In order to verify the accuracy of the models, three additional formulae

Table 1
Slag XRF (wt.%). One sample was analyzed; errors shown are typical relative accuracies for each element, as determined by calibration.

CaO	SiO_2	Al_2O_3	MgO	SO_3	TiO_2	Fe_2O_3	Na_2O	MnO	K_2O
39.4 ± 4.0	38.4 ± 0.8	12.9 ± 1.4	6.2 ± 1.0	2.1 ± 1.1	0.4 ± 0.0	0.4 ± 0.1	0.2 ± 0.0	0.4 ± 0.1	0.2 ± 0.0

Table 2
Cost, CO_2 production, and DOE mixture boundaries. Calculations for CO_2 and energy are provided in Appendix A.

Material	Cost/tonne	CO_2 produced (kg/tonne)	Energy consumed (kW h/tonne)	DOE mixture boundaries	
				Constraints	Resulting ranges, total wt.%
GGBFS	$80.00 [36,37]	28.8	47.2	25–80% of total weight	25–56
Limestone	$8.60 [38]	12.2	20.1	25–80% of total weight	25–56
Na_2CO_3	$105.00 [39]	110.8	374.1	25–100% of slag + limestone	4–35
Water	–	–	–	18–25% of dry components	15–20

Table 3
Formulations and responses. Formulations and responses are given for all 22 DOE runs. Confidence in the data in this table is presented as follows: mix design, cost, CO_2: none, since this is theoretically derived (normalized to a batch size of 1000 g), compressive strength and ASTM C469 chord modulus: (mean) ± [(1 standard deviation of 3 samples) + (1.5% system accuracy measured by calibration)], Δ Weight: ±1 standard deviation of 3 samples. Superscripts on run letters indicate replicate groups. Blank entries indicate that data was either impossible to obtain (e.g. no modulus test was performed for samples with negligible strength) or insufficient for a reliable reading.

Run	Point type	Mix design (g)				Cost ($/tonne)	CO_2 produced (kg/tonne)	Energy consumed (kW h/tonne)	Compressive strength (MPa)				ASTM C469 chord modulus (GPa)				Δ Weight (%)			
									Moist curing		Submerged curing		Moist curing		Submerged curing		Moist curing		Submerged curing	
		Slag	Na_2CO_3	Limestone	Water				3 d	28 d	3 d	28 d	3 d	28 d	3 d	28 d	3 d	28 d	3 d	28 d
A	Axial check blend	428.4	86.1	297.4	188.1	$56.49	31.9	72.8	46.7 ± 3.8	60.9 ± 3.5	49.3 ± 5.9	58.8 ± 3.2	15.9 ± 0.4	14.4 ± 0.3	15.2 ± 0.8	14.1 ± 0.4	0.4 ± 0.0	0.3 ± 0.0	0.1 ± 0.0	0.5 ± 0.0
B	Vertex	250.0	38.1	511.9	200.0	$35.50	22.6	46.3	17.4 ± 0.8	30.6 ± 1.1	16.9 ± 0.5	31.2 ± 0.8	9.8 ± 1.0	–	8.3 ± 0.6	8.8 ± 0.6	0.2 ± 0.0	0.3 ± 0.0	0.0 ± 0.0	0.4 ± 0.0
C[a]	Center edge	250.0	193.9	403.5	152.5	$51.72	40.2	110.0	24.3 ± 2.1	38.2 ± 2.2	17.6 ± 0.6	2.6 ± 0.1	13.8 ± 0.7	–	7.2 ± 10	–	1.8 ± 0.2	0.3 ± 0.0	−1.0 ± 0.0	−3.6 ± 0.1
D	Center edge	381.0	169.0	250.0	200.0	$62.97	41.4	108.7	12.2 ± 0.8	48.0 ± 6.0	13.3 ± 0.8	40.2 ± 3.3	9.1 ± 0.7	14.1 ± 0.8	6.9 ± 0.5	–	1.2 ± 0.1	0.9 ± 0.1	−0.4 ± 0.0	−1.8 ± 0.1
E	Center edge	250.0	169.0	381.0	200.0	$51.28	38.7	104.3	19.5 ± 1.3	53.6 ± 2.1	19.5 ± 1.7	1.8 ± 0.1	11.6 ± 1.0	13.9 ± 0.9	9.8 ± 1.3	–	1.3 ± 0.1	0.3 ± 0	−0.3 ± 0.0	−3.9 ± 0.3
F	Center edge	381.0	38.1	381.0	200.0	$47.19	25.3	50.8	26.8 ± 1.0	43.9 ± 4.9	29.4 ± 1.9	41.6 ± 4.3	14.7 ± 0.5	12 ± 0.7	9.8 ± 1.3	11.2 ± 0.9	0.5 ± 0.0	0.7 ± 0.1	0.5 ± 0.0	0.9 ± 0.1
G	Vertex	557.1	40.4	250.0	152.5	$60.13	28.3	55.7	18.7 ± 10.2	25.7 ± 16.8	26.3 ± 18.9	31.1 ± 21.9	–	–	–	–	2.3 ± 1.3	2.6 ± 1.7	2.4 ± 1.7	2.5 ± 1.7
H	Center edge	403.5	40.4	403.5	152.5	$47.19	25.3	50.8	35.6 ± 10.7	57.7 ± 3.4	33.1 ± 4.1	51.2 ± 7.7	14.2 ± 1.6	14.9 ± 0.9	15.2 ± 0.3	14.0 ± 1.2	0.5 ± 0.2	0.6 ± 0.0	0.0 ± 0.0	0.6 ± 0.1
I	Vertex	250.0	152.5	40.4	557.1	$34.25	22.3	45.9	33.3 ± 1.9	49.0 ± 1.2	27.2 ± 2.7	46.2 ± 1.8	14.1 ± 0.9	15.2 ± 0.6	11.5 ± 0.2	13.9 ± 0.3	–	–	–	–
J	Axial check blend	297.4	188.1	217.0	297.4	$60.53	45.1	125.6	11.5 ± 0.2	35.7 ± 0.5	14.0 ± 0.2	10.7 ± 0.2	–	–	–	–	–	–	–	–
K	Axial check blend	297.4	188.1	86.1	428.4	$44.98	29.2	68.5	29.8 ± 2.0	52.5 ± 3.4	20.1 ± 1.5	34.3 ± 1.8	13.5 ± 1.0	13 ± 0.7	–	–	–	–	–	–
L[b]	Center	344.8	176.3	134.1	344.8	$54.18	35.7	90.0	20.0 ± 3.5	51.2 ± 9.4	17.0 ± 2.2	37.6 ± 10.0	12.8 ± 0.9	13.7 ± 0.6	8.6 ± 0.9	10.8 ± 1.1	1.6 ± 0.3	1.0 ± 0.2	0.0 ± 0.0	−0.7 ± 0.2
M[c]	Center edge	403.5	152.5	193.9	250.0	$64.66	43.2	114.9	19.2 ± 7.2	41.4 ± 7.6	11.9 ± 6.1	21.9 ± 3.6	–	–	–	–	2.4 ± 0.9	3.2 ± 0.6	1.4 ± 0.7	−0.2 ± 0.0
N[a]	Center edge	250.0	152.5	193.9	403.5	$51.72	40.2	110.0	17.9 ± 6.3	40.6 ± 1.2	18.5 ± 6.2	3.0 ± 0.5	10.9 ± 2.4	12.3 ± 0.5	10.7 ± 0.7	–	1.6 ± 0.6	1.2 ± 0.0	0.3 ± 0.1	−3.3 ± 0.5
O[d]	Vertex	250.0	152.5	347.5	250.0	$69.19	58.0	174.1	32.7 ± 0.6	0 ± 0	15.0 ± 3.9	0 ± 0	–	–	–	–	2.3 ± 0.0	–	−2.6 ± 0.7	–
P[c]	Center edge	403.5	152.5	193.9	250.0	$64.66	43.2	114.9	26.5 ± 7.9	29.1 ± 6.8	20.3 ± 10.8	21.0 ± 2.9	11.8 ± 0.9	10.2 ± 0.8	–	–	2.0 ± 0.6	1.5 ± 0.3	−0.4 ± 0.2	−2.2 ± 0.3
Q	Vertex	511.9	200.0	38.1	250.0	$58.88	28.0	55.2	35.8 ± 2.3	52.2 ± 5.7	28.9 ± 3.6	52.2 ± 1.1	13.5 ± 0.7	11.7 ± 0.6	12.4 ± 0.7	11.3 ± 1.1	0.4 ± 0.0	0.9 ± 0.1	0.6 ± 0.1	1.3 ± 0.0
R	Vertex	250.0	200.0	300.0	250.0	$67.06	54.9	162.2	12.8 ± 1.0	0 ± 0	9.3 ± 0.7	0 ± 0	–	–	–	–	0.9 ± 0.1	–	−2.9 ± 0.2	–
S[d]	Vertex	250.0	152.5	347.5	250.0	$69.19	58.0	174.1	25.6 ± 7.6	0 ± 0	13.1 ± 4.2	0 ± 0	–	–	–	–	2.0 ± 0.6	–	−2.6 ± 0.8	–
T[b]	Center	344.8	176.3	134.1	344.8	$54.18	35.7	90.0	34.5 ± 3.3	43.1 ± 4.2	25.0 ± 6.0	40.0 ± 2.5	13.5 ± 1.1	11.4 ± 0.4	9.4 ± 3.2	9.1 ± 0.2	1.0 ± 0.1	0.9 ± 0.1	−0.3 ± 0.1	−1.1 ± 0.1
U	Plane centroid	352.4	152.5	142.7	352.4	$54.52	36.2	91.9	38.3 ± 4.5	41.1 ± 4.6	34.2 ± 4.3	40.7 ± 3.7	13.6 ± 1.1	10.2 ± 0.4	11.2 ± 1.4	9.5 ± 1.4	1.1 ± 0.1	0.4 ± 0.0	−0.2 ± 0.0	−0.7 ± 0.1
V[b]	Center	344.8	176.3	134.1	344.8	$54.18	35.7	90.0	32.4 ± 5.6	47.9 ± 9.5	31.6 ± 5.1	40.9 ± 3.5	13.2 ± 0.9	10.6 ± 0.6	11.3 ± 1.5	8.8 ± 1.0	0.7 ± 0.1	0.5 ± 0.1	−0.4 ± 0.1	−0.7 ± 0.1
								Minimum	11.5	0.0	9.3	0.0	9.1	10.2	6.9	8.8	0.2%	0.3%	−2.9%	−3.9%
								Maximum	46.7	60.9	49.3	58.8	15.9	15.2	15.2	14.1	2.4%	3.2%	2.4%	2.5%
								Mean	26.0	38.3	22.3	27.6	12.9	12.7	10.5	11.2	1.3%	1.0%	−0.3%	−0.8%

were prepared, which were each optimized for different criteria. These three model validation formulations were moist cured and selected tests were performed.

3. Results

3.1. Direct observation

Formulae and responses for all DOE runs are provided in Table 3. Compressive strengths ranged from 9.3 ± 0.7 to 49.3 ± 5.9 MPa (1.35–7.15 ksi) at 3 d and from 0 to 60.9 ± 3.5 MPa (0–8.83 ksi) at 28 d. The ASTM C469 chord modulus of elasticity (measured between points of 50 micro-strain and 40% of the ultimate strength) ranged from 6.9 ± 0.5 to 15.9 ± 0.4 GPa (1000–2300 ksi) at 3 d and from 8.8 ± 0.6 to 15.2 ± 0.6 GPa (1300–2200 ksi) at 28 d.

As shown in Fig. 1, the various responses exhibited several independent trends. First, compressive strength and moduli correlate well (Fig. 1a). Compressive strength is given focus throughout, but the trends observed generally apply to the moduli as well. Second, there is no apparent correlation between material cost and strengths achieved (Fig. 1b), indicating that this system is one that could be optimized for performance in various applications, without necessarily increasing material cost. This would be unremarkable if material costs were comparable, but they vary by a factor of ~16, for example between limestone and Na_2CO_3. Third, weight loss during submerged curing, assumed to be from leaching of soluble salts, correlates to low compressive strengths (Fig. 1c). Strong differences between the two curing conditions were apparent in some mix designs but not others. For example, one formula achieved a 28 d compressive strength of 53.6 ± 2.1 MPa when moist cured, and 1.8 ± 0.1 MPa when cured submerged (Table 3, Run E). Conversely, one formula was 20% stronger when submerged instead of moist cured (Table 3, Run G). Fourth, weight loss when submerged also correlates with amount of Na_2CO_3 (Fig. 1d). That is, having excess Na_2CO_3 leads to weight loss, presumably due to leaching, and hence to poor strengths.

Other observations include:

- Increased compressive strength correlates with an increased proportion of GGBFS in the mix. Also apparent is that the higher proportion of GGBFS has more pronounced benefits at 28 d and for submerged curing than for 3 d or moist curing.
- Variations in strength are correlated to mass variations amongst the cylinders of each batch (both according to the standard deviations listed in Table 3). That is, high weight variations of the as-produced cylinders resulted in high variations in their

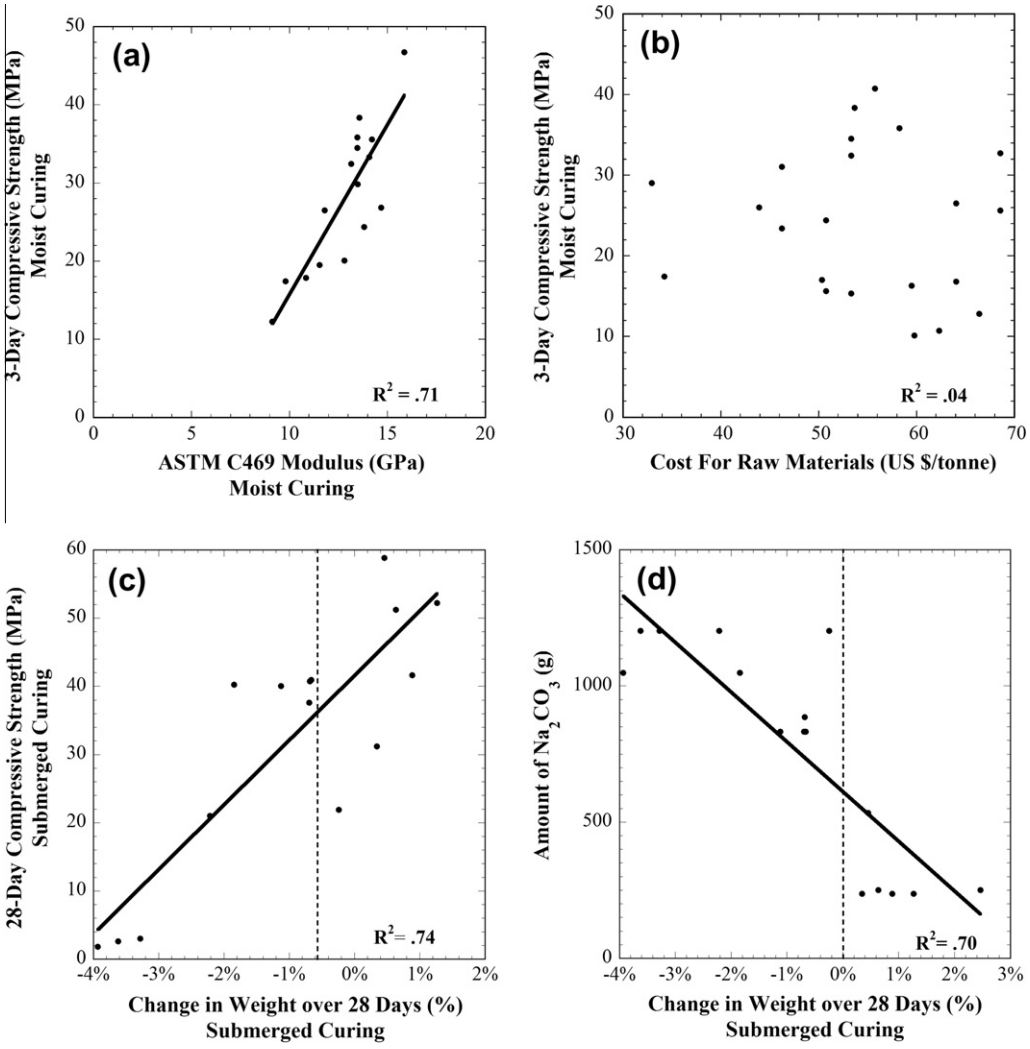

Fig. 1. Example mix and mechanical response correlations. Correlations (or lack thereof) between responses and/or mix components. See axis labels for the particular data set used. (a) Strength vs. modulus; (b) strength vs. cost (no correlation); (c) strength vs. change in weight; and (d) amount of Na_2CO_3 in mix vs. change in weight.

Table 4
Response models. Influence is marked as follows: major factors are indicated in green, moderate in yellow, and minor in blue.

					Model Terms											
#	Response	Units	Transform	R^2	A: Slag	B: Water	C: Soda Ash	D: Limestone	AB	AC	AD	BD	BC	CD	ACD	BCD
1	Comp. Str. 3 d Moist	MPa	Sqrt.	0.53	-4.207 x10^{-3}	-9.862 x10^{-3}	3.355 x10^{-3}	1.418 x10^{-3}	5.376 x10^{-6}		1.457 x10^{-6}					
2	Comp. Str. 3 d Submerged	MPa	Inv. Sqrt.	0.66	1.070 x10^{-4}	8.877 x10^{-5}	2.794 x10^{-5}	1.149 x10^{-4}			-8.542 x10^{-8}					
3	Comp. Str. 28 d Moist	MPa	Sqrt.	0.60	-2.902 x10^{-3}	1.265 x10^{-2}	-7.070 x10^{-4}	2.855 x10^{-3}			1.312 x10^{-6}	-5.261 x10^{-6}				
4	Comp. Str. 28 Day Submerged	MPa	None	0.81	2.452 x10^{-2}	8.832 x10^{-3}	-2.861 x10^{-2}	-3.116 x10^{-3}								
5	Modulus 3 d Moist	GPa	None	0.49	6.087 x10^{-3}	-6.328 x10^{-3}	7.120 x10^{-3}	3.006 x10^{-3}		-3.712 x10^{-6}						
6	Modulus 3 d Submerged	GPa	None	0.39	3.525 x10^{-3}	-1.726 x10^{-3}	-2.148 x10^{-3}	2.220 x10^{-3}								
7	Modulus 28 d Moist	GPa	None	0.84	-1.413 x10^{-2}	4.997 x10^{-2}	-4.581 x10^{-3}	1.139 x10^{-2}			4.229 x10^{-6}	-2.211 x10^{-5}				
8	Modulus 28 Day Submerged	GPa	None	0.88	-4.455 x10^{-2}	-1.575 x10^{-1}	1.035 x10^{-2}	3.065 x10^{-2}	7.913 x10^{-5}					9.454 x10^{-6}		
9	Str. Ratio 3 d (Sub./Moist)	%	Nat. Log	0.61	9.625 x10^{-4}	-1.154 x10^{-4}	-1.385 x10^{-3}	8.846 x10^{-4}					2.047 x10^{-6}			
10	Str. Ratio 28 d (Sub./Moist)	%	None	0.98	1.238 x10^{-1}	-2.296 x10^{-1}	-3.256 x10^{-1}	1.145 x10^{-2}		-1.775 x10^{-4}	-5.355 x10^{-5}	1.156 x10^{-4}	5.770 x10^{-4}	3.923 x10^{-5}	1.449 x10^{-7}	-2.773 x10^{-7}

KEY: Major | Moderate | Minor
Where only two levels are necessary, major and moderate are used.

Table 5
Model validation with optimized formulae. For moist curing condition. Error given for model prediction with respect to empirical data.

Run	% Error of model					
	Strength		Modulus		Δ Weight	
	3 d	28 d	3 d	28 d	3 d	28 d
V1 balanced, mod. flow	−4.6	−4.3	3.7	−9.4	136.1	9.3
V2 balanced, high flow	6.4	−2.1	14.8	−15.9	46.1	−20.6
V3 high strength	−7.2	−15.5	10.6	−12.4	56.5	19.8

strengths. This mass variability is likely due to two related factors: workability of the cement (fluidity, adhesion, set time, etc.) and how consistently the cylinders were packed.

- Successful formulae had up to 66 wt.% limestone (i.e. Run 1), far exceeding current regulatory limits for limestone-OPC blends.
- Cost, CO_2 production, and embodied energy are significantly less than for OPC. This is later improved upon through optimization (Section 3.3), and explained in more detail (Section 4). Limiting the use of Na_2CO_3 is beneficial, since it is highest in cost and CO_2 footprint (the latter by an order of magnitude with respect to limestone and GGBFS).

3.2. DOE modeling and validation

Mathematical models were derived with the DOE software, using the methods described above, and are reported in Table 4. The units, transform applied, coefficients of determination, R^2 values, and coefficients for each of 12 responses are listed, so that the models can be reconstructed with an understanding of the confidence level in each. Coefficients are marked as to how strongly they influence the model, as determined by the 'pseudo' coding internal to the DOE model generation. The presence of binary and tertiary terms indicate a high probability of interaction between those components. Responses 1–4 are the directly measured compressive strengths for each combination of curing conditions: moist or submerged and 3 d or 28 d. for a total of four responses. Responses 5–8 are the same, but for the moduli. Responses 9 and 10 are the ratio of the submerged and moist compressive strengths at 3 d and 28 d, respectively. For example, a value of 120 would indicate that the submerged sample was 20% stronger than the moist cured sample. This response would thus indicate hydraulic behavior, or lack thereof.

The models are constructed so that, provided the amount of each component in grams within the boundaries of Table 2, the predicted response is generated. Details and an example can be found in Appendix B.

In Table 5, models are validated by comparing results for three optimized formulae and the predicted responses (more on these formulae in Section 3.3). Most responses agree well, except for change in weight at 3 d. This is likely due to the relative sensitivity of the test to factors that are challenging to control, such as the exact amount of moisture lost from samples in the time between removal from the curing condition and weighing, and the higher variations at early ages in general.

3D response surfaces, such as shown in Fig. 2, were used to visualize the models. Based on Fig. 2a, in order to ensure good hydraulic behavior (defined here as the ratio of submerged to moist cure strengths), the Na_2CO_3 must be at a low level and the GGBFS at a relatively high level. A local maximum can be seen on this surface; formulae on this apex would be best for hydraulic curing. Fig. 2b provides a confirmation that a high amount of GGBFS, low water, and moderate Na_2CO_3 are ideal for strength. It was observed, however, that for some low levels of water, the mixture was difficult to work with and set rapidly. Further, excess Na_2CO_3 produces poor hydraulic stability (Fig. 2a). Thus, these and other practical matters must be considered when choosing a mix design.

3.3. Optimization

Finally, the response models were used to optimize the mix design for desired responses. Table 6 shows the mix design and responses for the three model validation formulae-referenced in Table 5 – compared to OPC. Optimization for the two "balanced"

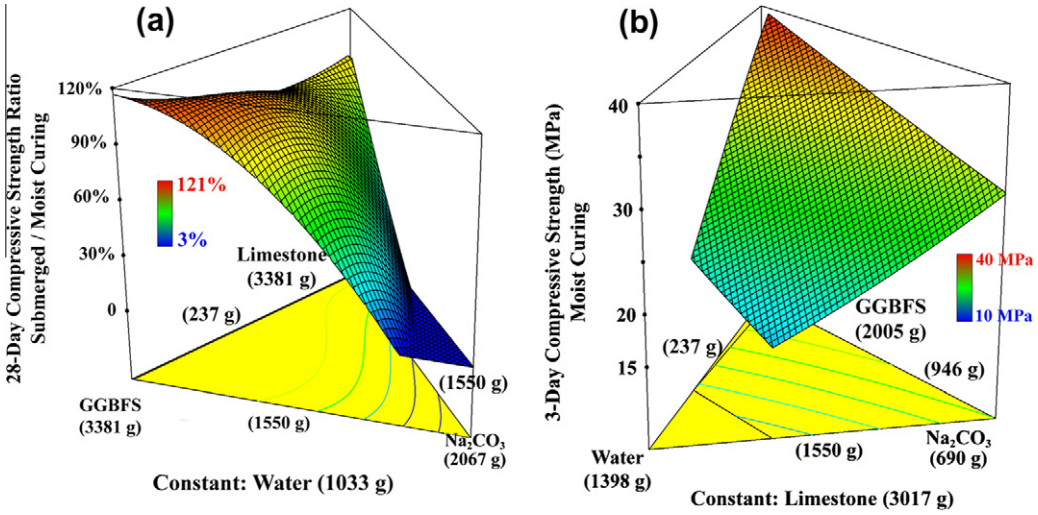

Fig. 2. Example response surface models. Response surface models (RSMs) for (a) compressive strength ratio at 28 d and (b) strength at 3 d. Note that the bottom plane behaves as a ternary diagram, with high amounts of the indicated component at the corners, and low amounts at the opposite side. One of the four components is kept constant, and each valid mixture sums to 6200 g (ranges shown in parenthesis) and obeys the boundaries set in Table 2. The *Y*-axis shows the response for the mixture.

Table 6
Optimized formulae, compared to OPC. Mix designs have been normalized to 1000 g. Confidence in the experimental data was calculated as for Table 3.

Formula	Mix design (g)				Cost ($/tonne)	CO_2 produced (kg/tonne)	Energy consumed (kW h/tonne)	Strength (MPa)	
	Slag	Na_2CO_3	Limestone	Water				3 d	28 d
Typical OPC	–	–	–	–	$102.00[a] [2]	898 (Appendix A)	1510 (Appendix A)	–	62–119 [40]
Balanced 1 (V1)	250	40	557	153	$34.30[b]	22.3	45.8	32.5 ± 0.4	51.0 ± 1.7
Balanced 2 (V2)	273	39	512	176	$36.80[b]	22.9	46.9	25.0 ± 0.6	44.3 ± 1.1
High strength (V3)	395	40	412	153	$46.50[b]	25.1	50.5	42.0 ± 0.7	64.1 ± 1.0

[a] Retail cost.
[b] Prices for materials only, FOB production plant. For cost assumptions, see Table 2.

formulae (V1, V2) was as follows: equal weight assigned to maximizing strength at all ages and curing conditions, minimizing cost, and having positive weight change (an indicator of hydraulic behavior). The second balanced formula (V2) had a higher flow than the first, measured qualitatively using a modified mini slump test, and due primarily to having more water and less GGBFS in the mix than formula V1. Optimization for high strength formulae (V3) was the same as for V1, except that no criterion was established for cost. This resulted in 28 d strength 4.5% higher than any of the original test runs, proof of the value of DOE and optimization. CO_2 production was also considered for optimization, but this was dependent almost entirely on the amount of Na_2CO_3. The latter was already at, or very near to, the minimum for the optimized runs. For the boundaries used, it thus did not require separate consideration [2,40].

4. Discussion

It is rare for the limestone proportion to reach the 35 wt.% limit of current standards, and levels above that rarer still. Thus, the success of formulae comprising up to 68 wt.% limestone (i.e. Table 6, formula V3) is significant. A survey of the literature yielded only two other investigations of greater than 35 wt.% limestone. The first comprised up to 58 wt.% limestone along with OPC, GGBFS, super-plasticizer, and polyvinyl alcohol fiber, with strengths up to 38 MPa at 28 d [41]. The second comprised up to 60 wt.% limestone along with gypsum, GGBFS, and steel slag, with strengths up to 30 MPa at 28 days (18 MPa for 60% limestone) [42]. In comparison, here, a 70% higher strength was achieved, with significantly more limestone and no need for OPC, super-plasticizer, or fiber.

Comparisons can also be drawn between this and other AACs. For example, Wang et al. achieved a 28 d strength of up to 36 MPa using Na_2CO_3 as the activator and up to 98 MPa (14.4 ksi) using 2 M waterglass solution [27]. The strength for Na_2CO_3 activation is significantly lower than that reported here, and waterglass, while stronger, is expensive and difficult to use in comparison to the Na_2CO_3. Hardjito et al. achieved a 7 d strength of 82 MPa (11.9 ksi) using a NaOH activated fly-ash cement, however, it required up to 100 h of curing at 60 °C [43]. NaOH is not as shelf-stable as Na_2CO_3 and curing at elevated temperatures is typically either costly, impractical, or both. Oh et al. achieved a 28 d strength of up to 50 MPa, but used NaOH or waterglass and cured at 80 °C [44].

The present work uses a shelf-stable activator and does not require curing at elevated temperatures, making it more practical for commercial use. Further, a patent claims the combination of calcium carbonate and sodium carbonate each in the range of 20–80 wt.%, plus up to 5 wt.% of other materials, but little data is available on it and tests performed by the authors showed those mixtures to have negligible strength [45]. It would appear that the novel addition of GGBFS to that mixture, well above levels covered in the patent, is necessary for success.

The use of DOE greatly benefitted the study and could help to overcome a challenge common to AACs. OFAT testing may have missed the ratio ranges for success. For example, seeing only Run E (Table 3) may have led one to erroneously conclude that the system is not hydraulically stable. Not only did the DOE reveal suc-

Table 7
Comparison of CO_2 and energy burden of cements.

Cement	CO_2 produced (kg/tonne)		Energy consumed (kW h/tonne)	
	Value	Reduction from OPC	Value	Reduction from OPC
OPC (Appendix A)	897	–	1510	–
OPC with CO_2 sequestration in cement kiln dust (CKD) [5]	837	7%	1510	0%
Blended Cement: 70% OPC, 30% GGBFS or fly ash	637	29%	1072	29%
High volume limestone AAC (V3, Table 6)	24.6	97%	50.5	97%

cessful ranges, but it allowed a number of observations to be made that require an understanding of the interaction of factors, such as those described in Sections 3.1 and 3.2. DOE also enabled optimization of strength, cost, and CO_2, yielding for example a formula 4.5% stronger at 28 d than any of the DOE runs (formula V3, Table 6). Further, variation in (often waste stream) raw materials is a problem common to AACs [22], which DOE could help to overcome. Models within, and between, studies could be developed to account for variation, allowing for rapid product development, customization, and robust quality control.

Further, the system presented here has clear ecological advantages in comparison with competing systems (Table 7). Optimized formula V3 (Table 6) uses 68 wt.% limestone and, compared to OPC, reduces both the CO_2 and energy burden by 97% while remaining competitive in performance. It also greatly surpasses the potential ecological advantage of two other strategies: CO_2 sequestration and blended cements. In fact, one businessperson familiar with the work remarked that, because no further thermal processing is required, we had developed "a way to make bread without an oven." Further, the materials used here are readily available, low cost, and practical (e.g. low-grade granular limestone, shelf-stable).

Finally, cement is most commonly used in concrete, so that is considered here as well. Comparing formula V3 (Table 6) directly to OPC, CO_2 production and energy consumption are both reduced by 97%. If this AAC were used for a typical ready-mix concrete mixture at the same proportion as OPC (a possibility, as confirmed by laboratory testing), the reduction in CO_2 production would be 93% (Appendix A). Thus, even in practical use, the AACs presented here would have a significant impact.

5. Conclusions

It has been shown that cements using only GGBFS, Na_2CO_3, water and up to 68 wt.% granular limestone can be cost- and performance-competitive with OPC. Further, greenhouse gas production and energy consumption are drastically reduced, the raw materials are widely available, and the cement is shelf-stable, hydraulically stable, and cures at room temperature. An optimized formula producing ~25 kg CO_2/tonne and requiring ~50 kWHs/tonne, represents 97% reductions in both CO_2 and energy compared to OPC, and 93% reductions for a typical concrete mix. Material costs for optimized mixtures are ~$32–$45/tonne, so it could be sold at a discount to OPC, primarily benefitting consumers, or sold at a premium for its ecologically benign characteristics, primarily benefitting producers. If used as a replacement for OPC in typical concrete, formula V3 (Table 6) could save 40% on cost and 93% on CO_2 and energy. The method used to reach these conclusions is equally important, as there exist only certain mixture combinations that yield desirable performances. DOE was employed for systematic design, analysis, optimization, and robustness, while requiring fewer runs than other methods such as OFAT.

Recommended future work includes measuring additional responses, application testing, reducing the Na_2CO_3 boundaries, and other further investigation of high volume limestone AACs. An investigation by the authors into the chemical nature of the system investigated here will be published separately.

Acknowledgements

The authors wish to acknowledge St. Lawrence Cement for the provision of slag, Drexel University collaborators Dr. Eva Jud Sierra, Aaron Sakulich and Sean Miller, Profs. Frank Moon, Grace Hsuan, and Sabrina Spatari, and the constructive criticism of anonymous reviewers. The primary author was supported successively by a Department of Education GAANN Fellowship and a National Science Foundation (NSF) Graduate Research Fellowship (GRFP). This work was funded by the Ceramics Division of NSF (DMR 0907430) and the EPA P3 program (SU834350). Although the research described in this article has been funded in part by the United States Environmental Protection Agency through grant/cooperative agreement SU834350 to Drexel University, it has not been subjected to the Agency's required peer and policy review and therefore does not necessarily reflect the views of the Agency and no official endorsement should be inferred.

Appendix A. CO_2 production and energy consumption calculations

Data for CO_2 production and energy consumption of OPC, GGBFS, and granular limestone was derived primarily from Worrell et al.'s 2001 *Carbon Dioxide Emissions From The Global Cement Industry* [1]. To calculate the CO_2 from the electricity used in each process step, the US average from the generation of electric power was used: 0.61 kg CO_2/kilowatt hour (kW h) [46]. The energy consumed and CO_2 produced are thus (per tonne of OPC):

Process step	kW h/tonne	kg CO_2/tonne
Crushing	0.9	0.5
Raw meal grinding	19.2	11.7
Clinker kiln: energy	1443.0	355.7
Clinker kiln: process	–	500.0
Finish grinding	46.3	28.2
Blending	0.9	0.5
Total for OPC	1510.2	896.7

Blending was assumed to require as much energy as crushing. The energy for all steps is in the form of electricity, except for clinker kiln energy, which is thermal. The clinker kiln process CO_2 production is due to the chemical reaction:

$$CaCO_3 \rightarrow CaO + CO_2$$

For GGBFS it was assumed that only crushing and finish grinding steps were performed, and that the energy required was equivalent to the above. Similarly, for granular limestone it was assumed that only crushing and raw meal (typically the grinding step before the material would be fed into a kiln) grinding steps were performed. Thus, the energy and CO_2 for these materials are:

Material	kW h/tonne	kg CO2/tonne
GGBFS	47.2	28.8
Granular limestone	20.1	12.2

All energy and CO_2 associated with the pig iron process which creates GGBFS was allocated to the iron, not the GGBFS, as GGBFS is a waste product of iron making.

For soda ash (Na_2CO_3), it was assumed that it was derived from trona ($Na_2CO_3 \cdot NaHCO_3 \cdot 2H_2O$), the most common procedure in the United States. This requires that the mineral trona be mined, or extracted from a brine lake, crushed, and calcined. Subsequent processes include filtration, centrifugation, and drying. Calcination temperature is on the order of 200 °C [47].

The chemical heat of decomposition for forming Na_2CO_3 from trona is 66.0 kW h/tonne [48]. It was assumed that the CO_2 produced by this thermal energy is produced at the same rate as in cement production (0.25 kg/kW h) and the process steps requiring electricity can be approximated as requiring electricity equivalent to crushing and finish grinding. Thus, the values for Na_2CO_3 are:

Process step	kW h/tonne	kg CO2/tonne
Thermal	326.0	81.5
Electric (crush, centrifuge, dry, etc.)	48.1	29.3
Total for Na_2CO_3	374.1	110.8

To calculate the CO_2 emitted from the production of concrete, the CO_2 associated with each main component is estimated and then a weighted average calculated for a typical mix. It was assumed that coarse aggregate requires only crushing, and sand requires crushing and raw meal grinding, both at the same levels as listed in the first table above.

	OPC	Coarse aggregate	Sand
Mix proportion	14%	48%	38%
kg CO_2/tonne	896.7	0.5	12.2
kW h/tonne	1510.2	0.9	20.1

Weighted averages: 130.9 kg CO_2/tonne, 219.5 kW h/tonne.

And the same concrete using AAC Formula V3 (Table 6):

	AAC V3	Coarse aggregate	Sand
Mix proportion	14%	48%	38%
kg CO_2/tonne	25.1	0.5	12.2
kW h/tonne	50.5	0.9	20.1

Weighted averages: 8.4 kg CO_2/tonne, 15.1 kW h/tonne.

For all compositions, a blending step was included at the rate listed in the first table above.

These calculations consider only CO_2 emissions and energy consumption for processing of the raw material to a final product, so it is a gate-to-gate analysis as opposed to cradle-to-gate (which would include mining, transportation, etc.) or cradle-to-grave or cradle-to-cradle (which would additionally consider installation, recycling, disposal, etc.). The use of AAC can be considered identical to that for OPC and mining for limestone is performed in both the AACs here and for OPC. GGBFS requires transportation but not mining and would be transported for disposal if not for reuse. The additional transportation for reuse varies widely from local (negligible) to transcontinental (e.g. ~130 kg CO_2/tonne shipping from southern Italy to New York City, USA) and would have to be determined on a case-by-case basis. Thus, this remains a reasonable scope of analysis.

Appendix B. Interpretation of DOE models

The DOE models are constructed so that, provided the amount of each component in grams, the predicted response is generated. The amounts used must obey the constraints listed in Table 2, as the model is only valid within the boundaries of the tests performed, and transforms must be applied when generating the response. For example, an inverse square root transform such as that for response 2 (compressive strength at 3 d, submerged cured) indicates that the model takes the form of the following equation:

$$\frac{1}{\sqrt{\text{Response}}} = mA + nB + pC + qD + rAD \quad (1)$$

where on the right side, lowercase variables indicate coefficients and uppercase variables the amount of the corresponding component in grams. Terms with more than one component (i.e. AC) have a coefficient separate from that of the individual components (i.e. A, C), but the amount in grams is the product of the individual components (i.e. AC = A * C). As a numerical example using Eq. (1) and response 2, using a mixture of 1690 g GGBFS, 1095 g water, 260 g Na_2CO_3, and 3155 g limestone would result in a 3 d compressive strength, moist cured, of 27 MPa.

References

[1] Worrell E, Price L, Martin N, Hendriks C, Meida LO. Carbon dioxide emissions from the global cement industry. Ann Rev Energy Environ 2001;26:203.
[2] van Oss HG. 2008 Mineral commodity summaries: cement. United States Geological Survey (USGS); January, 2008.
[3] Phair JW. Green chemistry for sustainable cement production and use. Green Chem 2006;8(9):763–80.
[4] Damineli BL, Kemeid FM, Aguiar PS, John VM. Measuring the eco-efficiency of cement use. Cem Concr Compos 2010;32(8):555–62.
[5] Huntzinger DN, Eatmon TD. A life-cycle assessment of Portland cement manufacturing: comparing the traditional process with alternative technologies. J Cleaner Prod 2009;17(7):668–75.
[6] Thomas MDA, Cail K, Blair B, Delagrave A, Masson P, Kazanis K. Use of low-CO_2 Portland limestone cement for pavement construction in Canada. Int J Pave Res Technol 2010;3(Compendex):228–33.
[7] Yilmaz B, Olgun A. Studies on cement and mortar containing low-calcium fly ash, limestone, and dolomitic limestone. Cem Concr Compos 2008;30(3):194–201.
[8] Voglis N, Kakali G, Chaniotakis E, Tsivilis S. Portland-limestone cements. Their properties and hydration compared to those of other composite cements. Cem Concr Compos 2005;27(2):191–6.
[9] Ramezanianpour AA, Ghiasvand E, Nickseresht I, Mahdikhani M, Moodi F. Influence of various amounts of limestone powder on performance of Portland limestone cement concretes. Cem Concr Compos 2009;31(Compendex):715–20.
[10] Wang S-D. Review of recent research on alkali-activated concrete in China. Mag Concr Res 1991;43(154):29–35.
[11] Duxson P, Fernández-Jiménez A, Provis JL, Lukey GC, Palomo A, van Deventer JSJ. Geopolymer technology: the current state of the art. J Mater Sci 2007;42:2917–33.
[12] Komnitsas K, Zaharaki D. Geopolymerisation: a review and prospects for the minerals industry. Miner Eng 2007;20(14):1261–77.
[13] Wang S-D, Pu X-C, Scrivener KL, Prattt PL. Alkali-activated slag cement and concrete: a review of properties and problems. Adv Cem Res 1995;7(27):93–102.
[14] Shi C, Krivenko PV, Roy DM. Alkali-activated cements and concretes. London; New York: Taylor & Francis; 2006.
[15] Pacheco-Torgal F, Castro-Gomes J, Jalali S. Alkali-activated binders: a review: Part 1. Historical background, terminology, reaction mechanisms and hydration products. Constr Build Mater 2008;22(7):1305–14.
[16] Pacheco-Torgal F, Castro-Gomes J, Jalali S. Alkali-activated binders: a review. Part 2. About materials and binders manufacture. Constr Build Mater 2008;22(7):1315–22.

[17] Talling B, Brandstetr J. present state and future of alkali-activated slag concretes. In: third international conference on fly ash, silica fume, slag, and natural pozzolans in concrete. Trondheim, Norway;1989. p. 1519–45.
[18] Sakulich AR, Anderson E, Schauer C, Barsoum MW. Mechanical and microstructural characterization of an alkali-activated slag/limestone fine aggregate concrete. Constr Build Mater 2009;23(8):2951–7.
[19] Sakulich AR, Anderson E, Schauer CL, Barsoum MW. Influence of Si:Al ratio on the microstructural and mechanical properties of a fine-limestone aggregate alkali-activated slag concrete. Mater Struct 2010;43(7):1025–35.
[20] Sakulich AR, Miller S, Barsoum MW. Chemical and microstructural characterization of 20-month-old alkali-activated slag cements. J Am Ceram Soc 2010;93(6):1741–8.
[21] Sakulich AR. Characterization of environmentally-friendly alkali activated slag cements and ancient building materials. Philadelphia, PA: Drexel University; 2009.
[22] Fernandez-Jimenez A, Palomo JG, Puertas F. Alkali-activated slag mortars – mechanical strength behaviour. Cem Concr Res 1999:1313–21.
[23] Sonebi M. Factorial design modelling of mix proportion parameters of underwater composite cement grouts. Cem Concr Res 2001;31(11):1553–60.
[24] Srinivasan CB, Narasimhan NL, Ilango SV. Development of rapid-set high-strength cement using statistical experimental design. Cem Concr Res 2003;33(9):1287–92.
[25] Vuk T, Tinta V, Gabrovsek R, Kaucic V. The effects of limestone addition, clinker type and fineness on properties of Portland cement. Cem Concr Res 2001;31(1):135–9.
[26] Zhao FQ, Ni W, Wang HJ, Liu HJ. Activated fly ash/slag blended cement. Resour Conserv Recycl 2007;52(2):303–13.
[27] Wang S-D, Scrivener KL, Pratt PL. Factors affecting the strength of alkali-activated slag. Cem Concr Res 1994;24(6):1033–43.
[28] Flesher P. Environmental protection agency recognizes cement industry for continued improvements (News Release). URL; 2010. <http://www.cement.org/newsroom/EPA_Sector.asp> [accessed August 2010].
[29] ASTM C 204-07. Standard test methods for fineness of hydraulic cement by air-permeability apparatus. Philadelphia (PA): American Society for Testing and Materials; 2007.
[30] ASTM C 125-07. Standard terminology relating to concrete and concrete aggregates. Philadelphia (PA): American Society for Testing and Materials; 2007.
[31] ASTM C 219-07a. Standard terminology relating to hydraulic cement. Philadelphia (PA): American Society for Testing and Materials; 2007.
[32] ASTM C 192/192M-07. Standard practice for making and curing concrete test specimens in the laboratory. Philadelphia (PA): American Society for Testing and Materials; 2007.
[33] ASTM C 39/39M-09a. standard test method for compressive strength of cylindrical concrete specimens. Philadelphia (PA): American Society for Testing and Materials; 2009.
[34] ASTM C 1231/1231M-10. standard practice for use of unbonded caps in determination of compressive strength of hardened concrete cylinders. Philadelphia (PA): American Society for Testing and Materials; 2010.
[35] ASTM C 469-02e1. Standard test method for static modulus of elasticity and Poisson's ratio of concrete in compression. Philadelphia (PA): American Society for Testing and Materials; 2010.
[36] Popp A. Price of GGBFS, Personal Communication. St. Lawrence Cement (Producer of Grancem); 2008.
[37] van Oss HG. 2008 Mineral commodity summary: iron and steel slag. United States Geological Survey (USGS); 2008.
[38] Willett JC. 2009 Minerals yearbook: stone, crushed. United States Geological Survey (USGS); 2009.
[39] Kostick DS. 2008 Mineral commodity summary: soda ash. United States Geological Survey (USGS); 2008.
[40] Sandberg PJ, Doncaster F. On the mechanism of strength enhancement of cement paste and mortar with triisopropanolamine. Cem Concr Res 2004;34(6):973–6.
[41] Zhou J, Qian S, Sierra Beltran M, Ye G, van Breugel K, Li V. Development of engineered cementitious composites with limestone powder and blast furnace slag. Mater Struct 2010;43(6):803–14.
[42] Lin Z, Zhao Q. Strength of limestone-based non-calcined cement and its properties. J Wuhan Univ Technol 2009;24(3):471–5.
[43] Hardjito D, Wallah SE, Sumajouw DMJ, Rangan BV. On the development of fly ash-based geopolymer concrete. ACI Mater J 2004;101(6):467–72.
[44] Oh JE, Monteiro PJM, Jun SS, Choi S, Clark SM. The evolution of strength and crystalline phases for alkali-activated ground blast furnace slag and fly ash-based geopolymers. Cem Concr Res 2010;40(2):189–96.
[45] McNulty Jr WJ. Inorganic cementitious material. USPTO 6264,740, July 24; 2001.
[46] Carbon Dioxide Emissions from the Generation of Electric Power in the United States. US Department of Energy & US Environmental Protection Agency; July, 2000.
[47] General Chemical Industrial Products. Green River Soda Ash Facility. URL, 2011. <http://www.genchem.com/pdf/Green%20River%20Soda%20Ash%20Facility.pdf> [accessed August 2011].
[48] Solvay Chemicals Technical Publication: Heat Effects of the Trona System. URL; 2011. <http://www.solvaychemicals.us/static/wma/pdf/6/8/3/6/HeatEffects_of_the_TronaSystem.pdf> [accessed August 2011].